



Chemosensitizing acridones: In vitro calmodulin dependent cAMP phosphodiesterase inhibition, docking, pharmacophore modeling and 3D QSAR studies

V.V.S. Rajendra Prasad^a, G. Deepak Reddy^a, D. Appaji^a, G.J. Peters^b, Y.C. Mayur^{c,*}

^a Medicinal Chemistry Research Division, Vishnu Institute of Pharmaceutical Education and Research, Narsapur, India

^b Department of Medical Oncology, VU University Medical Center, Amsterdam, The Netherlands

^c Department of Pharmaceutical Chemistry, Dr. Bhanuben Nanavati College of Pharmacy, Mumbai, India

ARTICLE INFO

Article history:

Accepted 17 December 2012

Available online 8 January 2013

Keywords:

Acridone

AHPRRR

3D-QSAR

Pharmacophore

Docking

Calmodulin

ABSTRACT

Calmodulin inhibitors have proved to play a significant role in sensitizing MDR cancer cells by interfering with cellular drug accumulation. The present investigation focuses on the evaluation of in vitro inhibitory efficacy of chloro acridones against calmodulin dependent cAMP phosphodiesterase (PDE1c). Moreover, molecular docking of acridones was performed with PDE1c in order to identify the possible protein ligand interactions and results thus obtained were compared with in vitro data. In addition an efficient pharmacophore model was developed from a set of 38 chemosensitizing acridones effective against doxorubicin resistant (HL-60/DX) cancer cell lines. Pharmacophoric features such as one hydrogen bond acceptor, one hydrophobic region, a positive ion group and three aromatic rings i.e., AHPRRR have been identified. Ligand based 3D-QSAR was also performed by employing partial least square regression analysis.

© 2013 Elsevier Inc. All rights reserved.

1. Introduction

The tumor microenvironment contributes to the development of multi-drug resistant (MDR) cancer and affects a patient's response to treatment, where the response of some tumors to cytotoxic/cytostatic drugs is very low and others initially respond well but eventually become resistant, with the possible emergence of resistant tumor cell subclones [1]. Multidrug resistance (MDR) is the phenomenon in which development of resistance towards one drug is accompanied by another molecule that might be structurally dissimilar [2]. Detoxifying systems, such as DNA repair and the cytochrome P450 mixed function oxidases also have their role to play in multidrug resistance [3]. Along with genetic mutations of the cellular structures and detoxifying systems, drug resistance occurs through expression of some special ATP-dependent pumps such as P-glycoprotein (P-gp) and multidrug resistant associated proteins (MRPs) which pumps out the cytotoxic chemicals from the cell for its survival. These efflux pumps belong to the ATP binding cassette (ABC) transporters family sharing sequence and structural similarities [4,5]. Liver, kidney and intestine are the common sites

of most of these transporters and some are also present in brain and its components (ABCB1, ABCA2), prostate, testis, ovary (ABCC3). Most common chemotherapeutic agents that are effluxed by these proteins are doxorubicin, daunorubicin, vincristine, vinblastine and taxols [6–8]. P-gp and MRP1 are the most important drug efflux proteins, which utilize the energy of ATP hydrolysis to translocate a wide range of substrates across a variety of cellular membranes [9]. Calmodulin is a vital component in the regulation processes, such as the assembly and disassembly of microtubules by controlling protein kinase activities, by exerting an indirect influence upon a wide variety of cellular processes. It is observed that the intracellular concentration of calcium in multidrug resistant cells is greater than non-resistant cells which contribute to their increased sensitivity to calmodulin antagonism compared with that of non-resistant cells. Calmodulin inhibitors have shown significant sensitizing property against MDR cells by interfering with cellular drug accumulation [10].

In recent years acridone containing molecules have proved to be effective chemosensitizing agents in cancer. Our previously published results showed that various N¹⁰-substituted acridones have ability to revert doxorubicin resistance in different cancer cells [11–14]. Present investigations are focused on the structural insights of the acridones for their MDR reversal activity by identifying possible common pharmacophore features from which a ligand based 3D-QSAR model has been derived. Further molecular docking studies were performed for a set of chloro acridone

* Corresponding author at: Department of Pharmaceutical Chemistry, Dr. Bhanuben Nanavati College of Pharmacy, Vile Parle (W), Mumbai, India, Tel.: +91 9405233178; fax: +91 22 26132905.

E-mail address: mayuryc@hotmail.com (Y.C. Mayur).

derivatives against calmodulin dependent cAMP phosphodiesterase in order to identify the possible binding interactions. The results thus obtained were compared with their in vitro anti-calmodulin properties.

2. Materials and methods

2.1. In vitro inhibition of calmodulin dependent cAMP phosphodiesterase by chloro acridones

The assay mixture containing 25 mM Tris–HCl (pH 7.5), 25 mM imidazole (pH 7.5), 1.5 mM magnesium acetate, 2 μ M Ca^{+2} , 1.25×10^{-4} U phosphodiesterase and 0.043 μ mol of cAMP in a total of 0.15 ml, was incubated at 30° C for 30 min (1 U of enzyme activity is defined as the activity in the absence of calmodulin, which hydrolyzed 1.0 μ mol of 3',5'-cyclic AMP to 5'AMP min^{-1} at pH 7.5). Reaction was terminated by heating the reaction mixture in a boiling water bath for 2 min. Denatured proteins were removed by centrifugation at 10,000 rpm for 10 min and 100 μ l of supernatant was injected to HPLC. The amount of cAMP hydrolyzed by the enzyme was determined in terms of the amount of AMP formed, which could be estimated with the help of a previously obtained standard curve for AMP. Blank reactions were run concurrently with the test reaction for substrate blank correction.

The assay was carried out in the presence and absence of different concentrations of acridone derivatives, in the range 0.001–100 μ M, dissolved in DMSO. Before the reaction was started, 5 μ l of modulator was added to the assay mixture. Addition of an equivalent amount of 5 μ l of DMSO to the reaction mixture did not show any inhibitory effect on the calmodulin dependent cAMP phosphodiesterase. The results are expressed as the concentration of inhibitor giving 50% inhibition of the calmodulin dependent cAMP phosphodiesterase activity. The IC_{50} was determined from a plot of percentage activation versus varying concentrations of the modulator. To validate the phosphodiesterase assay method by HPLC, the IC_{50} value of 2-chlorpromazine was also determined.

2.2. Docking and post docking calculations

Protein ligand interactions of the chlorine containing acridones with calmodulin dependent cAMP-phosphodiesterase (PDE1c) enzyme were studied by employing an efficient docking protocol, GLIDE XP. Initially, a theoretically built digitalized structure of the protein PDE1C was retrieved from the protein databank with PDB ID: 1LXS. Structure of the protein was corrected by adding hydrogens to satisfy the valence and optimized by using OPLS-2005 force field (optimized potentials for liquid simulations). Binding pockets were identified by using the SITEMAP tool. Receptor grid generation was accomplished using Glide docking protocol and ligands were docked by employing XP mode of Glide. Best pose of each ligand was ranked according to the E-model energy. The docking score from Glide (Glide Score) is entirely based on Chem Score. It also includes a steric-clash term, adds polar terms featured by Schrodinger to correct electrostatic mismatches [15,16].

$$\text{GScore} = 0.065 \times \text{Van der Waals energy} + 0.130 \times \text{Coulomb energy} + \text{Lipophilic term (Hydrophobic interactions)} + \text{H bonding} + \text{Metal binding} + \text{BuryP (Penalty for buried polar groups)} + \text{RotB (Penalty for freezing rotatable bonds)} + \text{Site (Polar interactions in the active site)} \quad (1)$$

Post docking calculations for the docked complexes were performed by using Prime MM/GBSA (molecular mechanics based generalized born/surface area) module of Schrodinger suite. The Prime MM-GBSA approach in Schrodinger predicts the free energy

of binding for a given receptor and a set of given ligands. As the docking algorithms provide good quality binding sites, an energy function with a well-defined description of binding contributions was utilized to re-score the docking results. MM-GBSA approach is the combination of OPLS molecular mechanics energies (EMM), an SGB solvation model for polar solvation (GSGS), and a non-polar solvation term (GNP) containing non-polar solvent accessible surface area and Van der Waals interactions [17,18]. The total free energy of binding is then expressed in the form below mentioned equation:

$$\Delta G_{\text{bind}} = G_{\text{complex}} - (G_{\text{protein}} + G_{\text{ligand}}) \quad \text{where } \Delta G_{\text{bind}} \text{ is ligand binding} \quad (2)$$

2.3. Data set

A set of 38 N^{10} -substituted acridone derivatives which were previously designed, synthesized in our laboratory and screened for their in vitro cytotoxic effects (pIC_{50}) against doxorubicin resistant HL-60 cell lines (HL-60/DX), results thus obtained were selected for the present study [12–14]. The data set consists of inactive, intermediate and highly active molecules. Out of 38 molecules 80% was selected randomly as training set and remaining as test set for QSAR analysis. 2D molecular structures of the ligands along with QSAR activity data were shown in Table 1.

2.4. Ligand preparation

Molecules selected for the analysis were designed using Chem Sketch of Schrodinger suite 2012 and then subjected to geometrical optimization using Ligprep module. In this step, a single, low energy 3D structure was obtained for each ligand and many conformers/tautomers obtained during ionization of the ligands using EPIK module which generate ionization states at pH range of 7 ± 2 [19]. Molecular properties of the processed ligands were studied by using Qikprop module [20] and listed in Table S1 (supplementary data), which also predict ADME profiles like blockage of HERG K^+ channels [21], apparent Caco-2 cell permeability [22], brain/blood partition coefficient [23], apparent MDCK cell permeability [24], skin permeability [25], binding to human serum albumin [26], and human oral absorption [27] of the given set of ligands. Results of ADME predictions were tabulated in Table S2 (supplementary data).

2.5. Pharmacophore development and QSAR analysis

Common pharmacophore hypotheses (CPH) and 3D-QSAR models were generated by using Phase module of Schrodinger suite for the set of 38 acridone containing ligands selected from the previously published results from our laboratory [28]. All the ligands were categorized into active, intermediate and inactive according to the activity thresholds. To generate common pharmacophore hypotheses, maximum of six sites were selected in order to obtain an efficient model. The Phase activity provides a six set

pharmacophoric features, hydrogen bond acceptor (A), hydrogen bond donor (D), hydrophobic group (H), positively ionizable (P), negatively ionizable (N), and aromatic ring (R). Hypotheses were generated by a systematic variation of number of sites (n_{sites}) and

Table 1
Structures and QSAR activity data of MDR reversal acridone derivatives.

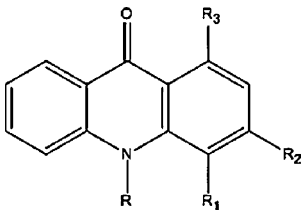
								
Compound no.	R	R1	R2	R3	pIC ₅₀ experimental	pIC ₅₀ predicted	Pharm set	Data set
1	—H	F	H	H	4.326	4.36	Inactive	Training
2	—CH ₂ —CH ₂ —CH ₂ —Cl	F	H	H	4.614	4.60	Inactive	Training
3	—(CH ₂) ₃ —N(CH ₂) ₆ —CH ₃	F	H	H	4.527	4.67	Inactive	Test
4	—(CH ₂) ₃ —N(CH ₂) ₆ —H	F	H	H	4.567	4.54	Inactive	Training
5	—(CH ₂) ₃ —N(CH ₂) ₆ —O—H	F	H	H	4.500	4.52	Inactive	Training
6	—(CH ₂) ₃ —N(CH ₂) ₆ —CH ₂ —CH ₂ —OH	F	H	H	4.790	4.79		Training
7	—(CH ₂) ₃ —N(CH ₂) ₅ —H	F	H	H	4.535	4.54	Inactive	Training
8	—(CH ₂) ₃ —N(CH ₂) ₂ —C ₂ H ₅	F	H	H	4.447	4.41	Inactive	Training
9	—(CH ₂) ₃ —N(CH ₂) ₂ —CH ₂ CH ₂ OH	F	H	H	4.785	4.71		Test
10	—CH ₂ —CH ₂ —CH ₂ —CH ₂ —Cl	F	H	H	4.921	4.90	Active	Training
11	—(CH ₂) ₄ —N(CH ₂) ₆ —CH ₃	F	H	H	5.076	5.10	Active	Training
12	—(CH ₂) ₄ —N(CH ₂) ₆ —H	F	H	H	4.971	5.15	Active	Training
13	—(CH ₂) ₄ —N(CH ₂) ₆ —O—H	F	H	H	5.432	5.26	Active	Training
14	—(CH ₂) ₄ —N(CH ₂) ₆ —CH ₂ —CH ₂ —OH	F	H	H	5.420	5.44	Active	Training
15	—(CH ₂) ₄ —N(CH ₂) ₅ —H	F	H	H	5.310	5.09	Active	Test
16	—(CH ₂) ₄ —N(CH ₂) ₂ —C ₂ H ₅	F	H	H	5.086	5.08	Active	Training
17	—(CH ₂) ₄ —N(CH ₂) ₂ —CH ₂ CH ₂ OH	F	H	H	5.310	5.31	Active	Training

Table 1 (Continued)

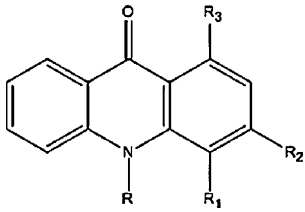
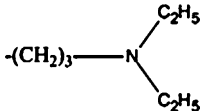
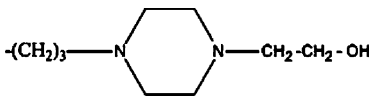
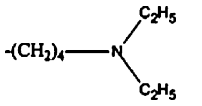
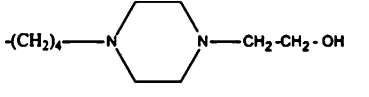
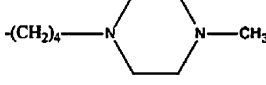
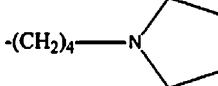
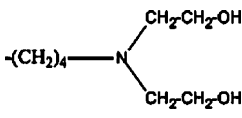
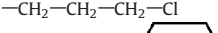
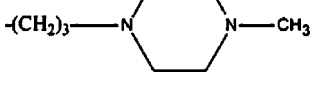
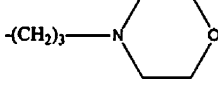
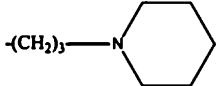
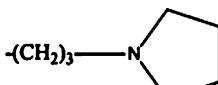
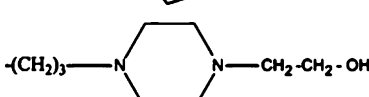
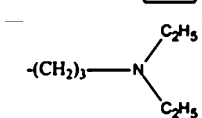
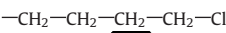
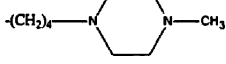
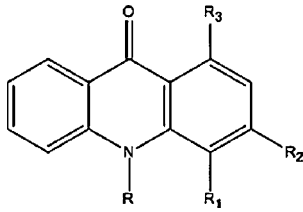
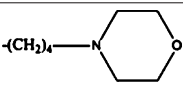
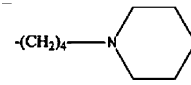
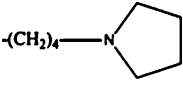
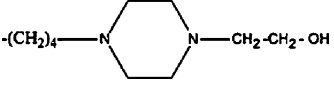
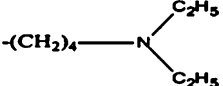
								
Compound no.	R	R1	R2	R3	pIC ₅₀ experimental	pIC ₅₀ predicted	Pharm set	Data set
18		Cl	H	H	5.127	5.15	Active	Training
19		Cl	H	H	4.968	4.99	Active	Training
20		Cl	H	H	5.745	5.54	Active	Test
21		Cl	H	H	5.969	5.98	Active	Training
22		Cl	H	H	5.558	5.53	Active	Test
23		Cl	H	H	5.687	5.69	Active	Training
24		Cl	H	H	5.585	5.58	Active	Training
25		H	COOCH ₃	COOCH ₃	4.730	4.72		Training
26		H	COOCH ₃	COOCH ₃	4.634	4.65		Training
27		H	COOCH ₃	COOCH ₃	4.804	4.79	Active	Training
28		H	COOCH ₃	COOCH ₃	4.917	4.96	Active	Training
29		H	COOCH ₃	COOCH ₃	4.959	4.95	Active	Training
30		H	COOCH ₃	COOCH ₃	5.060	5.04	Active	Training
31		H	COOCH ₃	COOCH ₃	4.991	4.80	Active	Test
32		H	COOCH ₃	COOCH ₃	5.337	5.29	Active	Training
33		H	COOCH ₃	COOCH ₃	5.092	5.14	Active	Test

Table 1 (Continued)

								
Compound no.	R	R1	R2	R3	pIC ₅₀ experimental	pIC ₅₀ predicted	Pharm set	Data set
34		H	COOCH ₃	COOCH ₃	5.215	5.20	Active	Training
35		H	COOCH ₃	COOCH ₃	5.161	5.09	Active	Training
36		H	COOCH ₃	COOCH ₃	4.954	5.02	Active	Training
37		H	COOCH ₃	COOCH ₃	4.882	4.87	Active	Training
38		H	COOCH ₃	COOCH ₃	5.574	5.58	Active	Training

the number of matching active compounds (n_{act}). With $n_{\text{act}} = n_{\text{act}} - n_{\text{tot}}$ initially ($n_{\text{act}} - n_{\text{tot}}$) is the total number of active compounds in the training set, n_{sites} . Atom based QSAR model has been developed by maintaining 1.00 Å and six partial least squares (PLS) factors, 31 of 38 ligands were randomly selected as training set ligands and remaining as test set ligands for internal validation.

The predictive value of the models was evaluated by leave-one-out (LOO) and leave-half-out (LHO) cross-validation. The cross validated coefficient, r_{cv}^2 , was calculated using the following equation.

$$r_{\text{cv}}^2 = 1 - \frac{\sum (Y_{\text{predicted}} - Y_{\text{observed}})^2}{\sum (Y_{\text{observed}} - Y_{\text{mean}})^2} \quad (3)$$

where $Y_{\text{predicted}}$, Y_{observed} , and Y_{mean} are the predicted, observed and mean values of the target property (pIC₅₀), respectively, $(Y_{\text{observed}} - Y_{\text{mean}})^2$ is the predictive residual sum of squares (PRESS). The predictive correlation coefficient (r_{pred}^2), based on molecules of test set, is defined as,

$$r_{\text{pred}}^2 = \frac{\text{SD} - \text{PRESS}}{\text{SD}} \quad (4)$$

where SD is the sum of the squared deviations between the biological activities of the test set and mean activities of the training set molecules, PRESS is the sum of squared deviation between predicted and actual activity values for every molecule in test set. According to the literature [29–31], 3D-QSAR models were accepted if they satisfy all of the following conditions:

$$r^2 > 0.6; \quad r_{\text{cv}}^2(q^2) > 0.5 \quad (5)$$

3. Results and discussions

To investigate the role of calmodulin in chemosensitizing properties of chloro acridones which were previously reported from

our laboratory [14], we have evaluated in vitro inhibitory ability of chloro acridones against calmodulin dependent cAMP phosphodiesterase (PDE1c) (Table 2). The results thus obtained were correlated with the data of in silico studies performed. Evaluation of anti-calmodulin activity is based on the measurement of phosphodiesterase activity in the presence or/and absence of chloro acridones. This method involves the hydrolysis of cAMP to AMP, a product of cAMP phosphodiesterase reaction, followed by quantitation by HPLC method. Minimum detection level of AMP by this method was 0.05 µg and was linear upto 3.15 µg ($R = 0.997$). In the absence of calmodulin, phosphodiesterase had a low basal activity of 0.062 µmol mg⁻¹ min⁻¹. In order to find out the substrate saturation point, cAMP was varied from 0.15 to 91.00 nmol in the reaction mixture containing 1.25×10^{-4} U of phosphodiesterase. K_m of the enzyme for cAMP was found to be 4×10^{-5} M and V_{max} was 326.8 nmol of AMP hydrolyzed mg⁻¹ min⁻¹ of protein. The hydrolysis of cAMP by the enzyme was studied as a function of incubation time and the rate of formation of AMP was linear for at least 90 min, after which the activity decreased presumably due to the decrease of the substrate concentration in the reaction mixture. The pH of the working buffer was also varied from 3 to 11 and an optimum pH of 7.5 was found maximum for enzyme activity, which closely approximates with previous results [32]. In order to determine the effect of calmodulin concentration for maximum phosphodiesterase activity, varied concentrations of activator upto 0.2 µg (0.0–1.0 U) were incubated with 1.24×10^{-4} U of phosphodiesterase containing 0.043 µmol of cAMP and the activity determined. The stimulation was low at less concentration of activator. As the concentration of the activator increased, the extent of stimulation was proportionately greater, reaching a plateau at 0.12 µg (0.6 U) of calmodulin. Half-maximal activation was obtained at 6.6×10^{-3} µg (0.033 U) of activator. With saturating concentration of the activator, the enzyme activity was stimulated approximately by five-fold. As activation of the enzyme was completely dependent on the addition of calmodulin and Ca²⁺, a 2.3 µM concentration of calcium was found

Table 2

In vitro, in silico inhibition of calcium/calmodulin dependent cAMP phosphodiesterase and protein ligand interactions of chlorine containing acridones with the target protein.

Compound ^b	PDE1c Inhibition IC ₅₀ (μM)	XP Gscore	No. of H bonds	Amino acids (interacted) ^a	Distance (Å)	Prime MMGBSA complex Energy	Prime MMGBSA ligand energy	Prime MMGBSA receptor energy	Prime MMGBSA DG bind
22	1.9	-8.58468	1	ASP 214	2.061	-12412.273	8.876984	-12359.349	-61.800454
19	1.7	-8.07366	2	ASP 214 MET 180	1.789 1.687	-12422.495	23.759844	-12359.349	-86.905512
24	1.5	-7.97707	2	GLU 136 ASP 107	1.837 1.723	-12433.202	13.897689	-12359.349	-87.750281
21	2.4	-7.36734	2	ASP 214 GLU 136	1.751 2.052	-12419.839	5.647475	-12359.349	-66.136893
20	4.7	-1.9428	1	HIE 66	1.822	-12403.259	9.228431	-12359.349	-53.138551
18	28.1	-1.65154	1	HIE 66	2.325	-12390.417	18.263703	-12359.349	-49.331085
23	9.4	-0.24138	–	–	–	-12386.165	29.089501	-12359.349	-55.904727

^a Codes for amino acids: ASP, aspartic acid; GLN, glutamine; MET, methionine; GLU, glutamic acid; THR, threonine; HIE, histidine.^b Acridones tabulated according to the XP Gscores.

to be essential for 50% of maximal activation and further demonstrated that Mg²⁺ cannot substitute for Ca²⁺ in the activation of the enzyme.

In the present HPLC method, AMP and cAMP were directly separated from the reaction mixture and quantitated to assay phosphodiesterase, calmodulin activation of phosphodiesterase and inhibition of calmodulin activation by chloro acridones. This method is simple, rapid, reproducible and a microassay to measure the activity of phosphodiesterase. This method offers numerous advantages over regularly used procedures, the major one being its great sensitivity. The calmodulin dependent enzyme inhibition properties were determined by assaying the phosphodiesterase activity in the presence or absence of chloro acridones in the range of concentration 0.001–100 μM and IC₅₀ values were determined from the dose response curves. Results indicate that none of the compounds had shown any significant inhibition of the calmodulin independent cAMP phosphodiesterase activity. These studies demonstrate that the chloro acridones inhibit the Ca²⁺/calmodulin stimulated cAMP–phosphodiesterase and have no direct effects on the enzyme itself. The IC₅₀ values lie in the range of 1.5–28.1 μM (Table 2) for 18–24 compounds. The most potent acridones among the derivatives screened was compounds 22 and 24 (Butyl side chain derivatives, IC₅₀ = 1.9 μM and 1.5 respectively) suggesting that the variation of the side chain is a strict requirement for cytotoxicity.

Possible protein ligand interactions of seven chlorine containing acridones with Ca²⁺/calmodulin stimulated cAMP phosphodiesterase (PDE1c) and binding modes of ligand in the binding pocket of the enzyme was identified by using Glide XP docking protocol of Schrodinger Suite. Protein ligand interaction studies have shown that the protein residues like ASP 214 is the common amino acid interacted with most of the ligands and other residues like ASP 107, GLN 265, GLU 136, HIE 66, and MET 180 also participated in the formation of hydrogen bonds. Structural insights of chloro acridones found that the compounds with butyl side chain at N¹⁰-position have shown good dock scores when compared with propyl derivatives. These results revealed that increase in length of side chain by one carbon at N¹⁰ position leads to slight rise in the dock score. Surprisingly, propyl derivative 19 showed greater dock score than butyl derivative 21. The reason is perhaps that the hydrogen bond distances are shorter in protein complex with compound 19 than that of compound 21, the shorter hydrogen bond distances increases energy and dock score. In addition the compound 23 does not possess any hydrogen bonding interactions with protein and this might be reason for the low dock score.

Dock scores, protein residues interacting with the ligands by hydrogen bond and their distances are tabulated in Table 2 according to their XP Gscores. Docking results thus obtained showed good

correlation when compared with experimental in vitro inhibitory properties of the chloro acridones against Ca²⁺/calmodulin stimulated cAMP–phosphodiesterase. Docking studies indicates that nitrogen containing substitution at R position (Table 1) plays a vital role in the hydrophilic interactions. Other groups like carbonyl (–C=O) at 9th position of acridone moiety showed significant role in ligand fitness at binding site of the enzyme. Docking conformation of the best fit ligand (compound 22) was shown in Fig. 1. Post docking calculations were performed by employing MM/GBSA to calculate the free energy of binding (FEB) of the ligand and the result was tabulated in Table 2. Components of ligand binding energies (Coulombic, covalent and van der Waals) are tabulated in Table S3 (supplementary data).

In order to identify and develop an efficient common pharmacophore, we have divided 38 molecules into active, intermediate and inactive based on pIC₅₀ values, pIC₅₀ values greater than 4.8 as active, between 4.6 and 4.8 as moderately active and the molecules with pIC₅₀ less than 4.6 as inactive. A set with maximum of six pharmacophoric features was selected to develop hypotheses and total of 10 common pharmacophoric hypotheses resulted for 38 ligands with similar pharmacophore features AHPRRR, one hydrogen bond acceptor (A), one hydrophobic group (H), one positively ionizable group (P), and three aromatic rings (R). Though the pharmacophoric features are same, the 3D spatial arrangements of the pharmacophoric features were found to be different. Spatial arrangement of common pharmacophoric hypothesis was shown in Fig. 2.

QSAR models have been built for all ten CPHs to identify the better pharmacophore model among the obtained sets as their survival scores were ranging between 3.326 (AHPRRR.658) and 3.126 (AHPRRR.654) and energies of these two systems were 5.687 and 4.968 respectively. QSAR results indicates that AHPRRR.518 hypotheses have shown best regression scores with R² of 0.98 and Q² of 0.86 by using partial least square analysis. Results of regression analysis of all other hypotheses are tabulated in Table 3. Another pharmacophore model of same compounds with same set of pharmacophoric features (AHPRRR.655) with different 3D spatial arrangement showed that 0.95 (R²), 0.87 (Q²) and 0.94 (Pearson-R).

The original set of molecules was segregated into training set of (31), and test set (7) randomly and the experimental, predicted pIC₅₀ values are summarized in Table 1. Ligands were aligned with the developed pharmacophore AHPRRR.518 and are depicted in Fig. 3. Distances and angles between all the pharmacophore points are tabulated in Tables S4 and S5 (supplementary data). Possible favorable and unfavorable regions of the ligands with respect to the developed pharmacophore model are explained by using counter maps (QSAR visualization). When all the ligands are aligned into the pharmacophore model hydrogen bond acceptor,

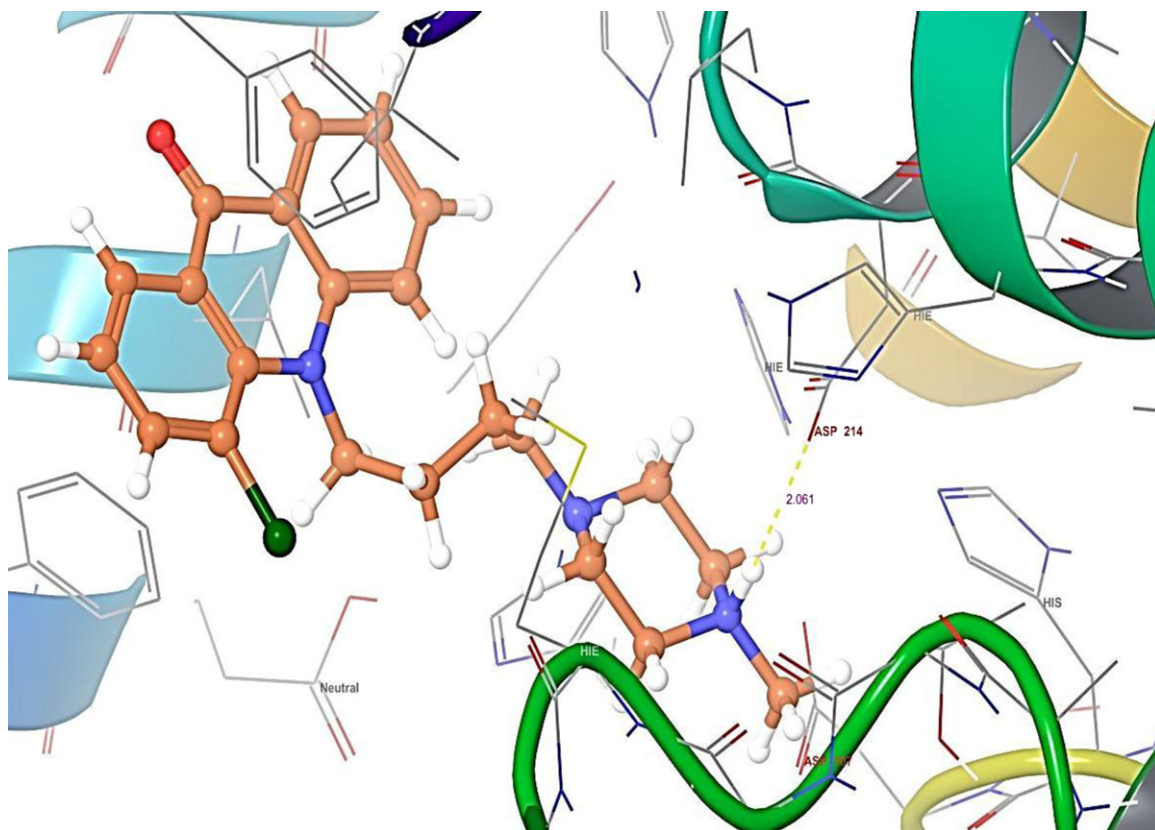


Figure 1. Binding orientations of compound 22 with Calcium/calmodulin-dependent cAMP phosphodiesterase enzyme.

*Compound 22 is showing 1 hydrogen bond with the protein residues (yellow colour dotted lines) Asp: Aspartic acid. (For interpretation of the references to color in this figure legend, the reader is referred to the web version of this article.)

aromatic ring, hydrophobic group and positively ionizable group regions are recognized as favorable regions, which can be seen in Fig. 3. In reference ligand nitrogen containing moiety at the side chain (positively ionizable group) is the most favorable

region for the fitness and activity. The QSAR regression analysis plots of actual activity (phase activity) vs. predicted activity is shown in Fig. 4 for training set ligands (inset) and for all ligands.

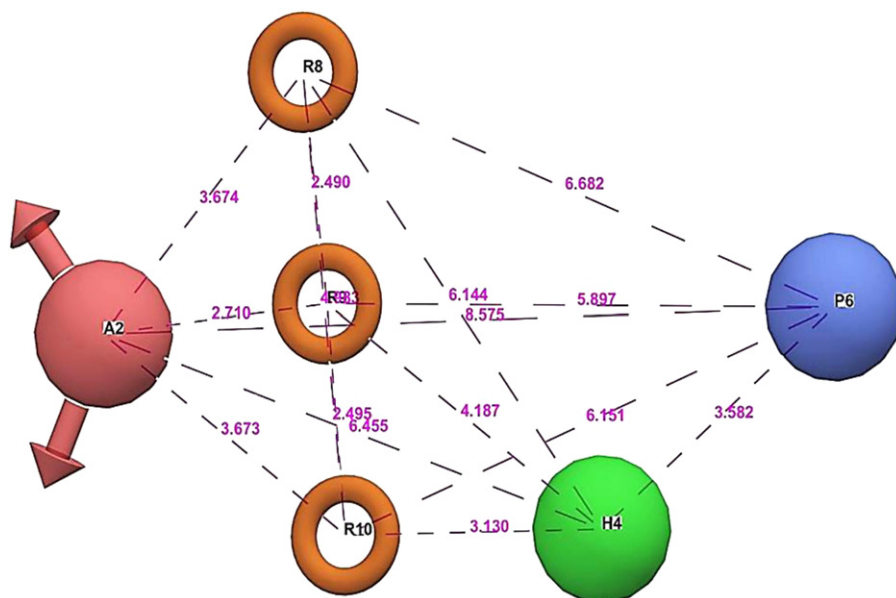


Figure 2. 3D spatial arrangement of the common pharmacophore AHPRRR.518 with inter pharmacophoric features distances. *Color coded pharmacophoric features: red, H-acceptor; orange aromatic ring; dark blue, positively charged group. Distances between pharmacophore features are reported in Angstroms.

Table 3
Scores of top ten hypotheses.

Hypothesis no.	Hypothesis	SD	R ²	F	RMSE	Q ²	Pearson-R
1	AHPRRR.518	0.0574	0.98	276.8	0.15	0.8563	0.9502
2	AHPRRR.655	0.0924	0.95	182.2	0.1822	0.8660	0.9390
3	AHPRRR.594	0.0975	0.95	154.4	0.1701	0.8213	0.9298
4	AHPRRR.652	0.0642	0.98	229.8	0.1683	0.7975	0.9479
5	AHPRRR.658	0.0678	0.98	201.8	0.1768	0.7956	0.9607
6	AHPRRR.589	0.0796	0.97	190.5	0.1687	0.7606	0.9123
7	AHPRRR.674	0.1075	0.94	132.9	0.1663	0.7789	0.8958
8	AHPRRR.593	0.1111	0.92	106.5	0.2247	0.7439	0.9334
9	AHPRRR.654	0.0655	0.98	218.6	0.2251	0.6482	0.8273
10	AHPRRR.588	0.0652	0.98	256	0.2611	0.6188	0.845

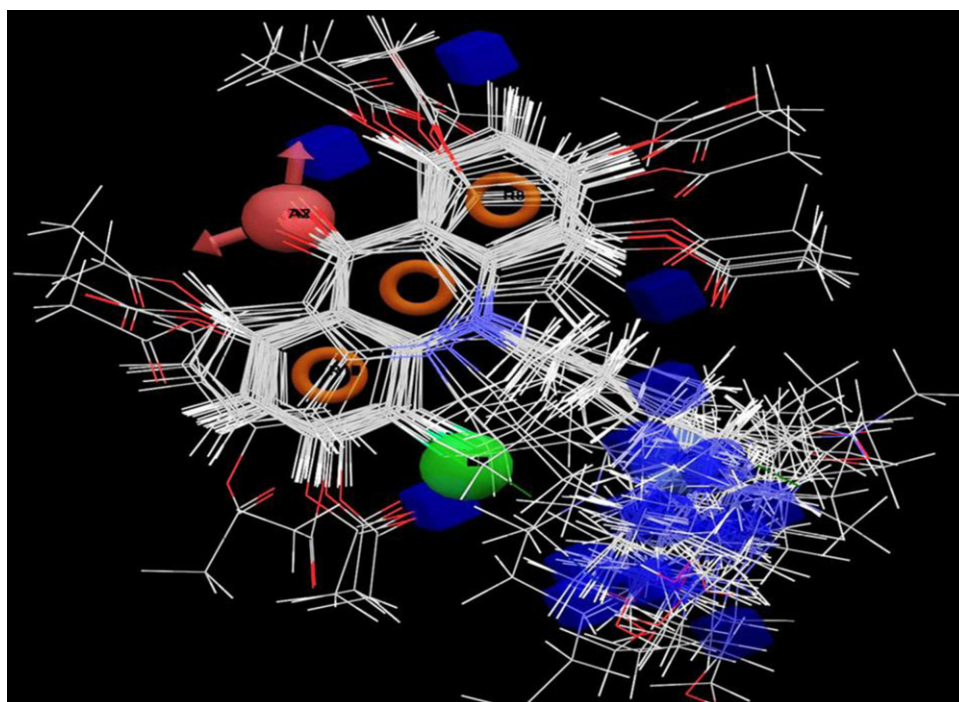


Figure 3. Ligand based alignment of 38 molecules in the data set. *Contour mapping for all 38 aligned molecules indicating favorable regions for interaction (blue color cubes). (For interpretation of the references to color in this figure legend, the reader is referred to the web version of this article.)

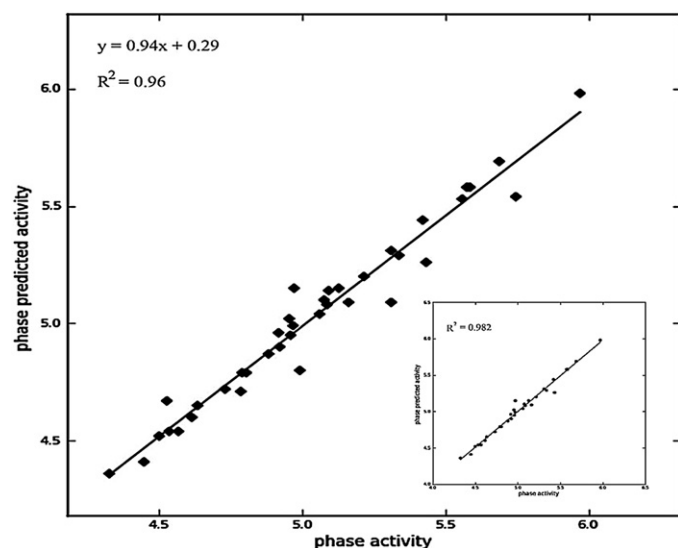


Figure 4. Fitness of predicted vs. actual pIC₅₀ for all data set molecules. *QSAR plots of predicted vs. actual pIC₅₀ for training set ligands were shown in inset.

4. Conclusions

In the present study, we attempted to identify the best suitable common pharmacophore for the acridone containing chemosensitizing agents applying ligand based approach by using PHASE module. The best hypothesis consists of six pharmacophore features with one hydrogen bond acceptor, one hydrophobic group, one positively ionizable group, and tricyclic aromatic rings, AHPRRR. Nitrogen containing side chain at R position is responsible for the formation of hydrogen bonds with protein residues; it might be a favorable region for the biological activity. Experimental *in vitro* calmodulin inhibition properties of acridones reveal that none of the compounds showed significant inhibition of the calmodulin independent cAMP–phosphodiesterase. The present investigation demonstrate that chloro acridones only inhibit the Ca²⁺/calmodulin stimulated cAMP–phosphodiesterase activity and have no direct effects on the enzyme itself. Results of ligand docking with calmodulin dependent cAMP phosphodiesterase (PDE1c) show that good correlation when compared with experimental *in vitro* data. We propose that the derived ligand based 3D-QSAR provides possible structural modifications for the strategic design of more potent chemosensitizing agents in cancer.

Acknowledgments

The financial assistance in the form of a “Fast Track Young Scientist Award” (SR/FT/LS-175/2009) to Dr. V.V.S. Rajendra Prasad from SERB, Department of Science and Technology (DST), Government of India, is gratefully acknowledged. We wish to acknowledge Sri Vishnu Educational Society (SVES) for the providing research facilities.

Appendix A. Supplementary data

Supplementary data associated with this article can be found, in the online version, at <http://dx.doi.org/10.1016/j.jmngm.2012.12.009>.

References

- [1] L.R. Ferguson, B.C. Baguley, Multidrug resistance and mutagenesis, *Mutation Research – Fundamental and Molecular Mechanisms of Mutagenesis* 285 (1993) 79–90.
- [2] R.J. Schepera, H.J. Broxterman, G.L. Scheffe, C.J.L.M. Meijer, H.M. Pinedob, Drug-transporter proteins in clinical multidrug resistance, *Clinica Chimica Acta* 206 (1992) 25–32.
- [3] E.G. Schuetz, W.T. Beck, J.D. Schuetz, Modulators and substrates of P-glycoprotein and cytochrome P4503A coordinately up-regulate these proteins in human colon carcinoma cells, *Molecular Pharmacology* 49 (1996) 311–318.
- [4] P.D. Roepe, The role of the MDR protein in altered drug translocation across tumor cell membranes, *Biochimica et Biophysica Acta* 1241 (1995) 385–405.
- [5] M. Dean, A. Rzhetsky, R. Alliknets, The human ATP-binding cassette (ABC) transporter superfamily, *Genome Research* 11 (2001) 1156–1166.
- [6] M.M. Gottesman, T. Fojo, S.E. Bates, Multidrug resistance in cancer: role of ATP-dependent transporters, *Nature Reviews Cancer* 2 (2002) 48–58.
- [7] S.V. Ambudkar, S. Dey, C.A. Hrycyna, M. Ramachandra, I. Pastan, M.M. Gottesman, Biochemical, cellular and pharmacological aspects of the multidrug transporter, *Annual Review of Pharmacology and Toxicology* 39 (1999) 361–398.
- [8] P. Borst, R. Evers, M. Koel, J. Wijnholds, A family of drug transporters: the multidrug resistance-associated proteins, *Journal of the National Cancer Institute* 92 (2000) 1295–1302.
- [9] E. Teodori, S. Dei, S. Scapecchi, F. Gualtieri, The medicinal chemistry of multidrug resistance (MDR) reversing drugs, *Farmaco* 57 (2002) 385–415.
- [10] T. Tsuruo, M. Iida, S. Tsukagoshi, Y. Sakurai, Increased accumulation of vincristine and adriamycin in drug-resistant P388 tumor cells following incubation with calcium antagonists and calmodulin inhibitors, *Cancer Research* 42 (1982) 4730–4733.
- [11] Y.C. Mayur, Zaheeruddin, G.J. Peters, C. Lemos, I. Kathmann, V.V.S. Rajendra Prasad, Synthesis of 2-fluoro N^{10} -substituted acridones and their cytotoxic studies in sensitive and resistant cancer cell lines and their DNA binding studies, *Archiv der Pharmazie – Chemistry in Life Sciences* 342 (2009) 640–650.
- [12] N.K. Sathish, V.V.S. Rajendra Prasad, N.M. Raghavendra, S.M. Shanta Kumar, Y.C. Mayur, Synthesis of novel 1,3-diacetoxy-acridones as cytotoxic agents and their DNA-binding studies, *Scientia Pharmaceutica* 77 (2009) 19–32.
- [13] V.V.S. Rajendra Prasad, G.J. Peters, C. Lemos, I. Kathmann, Y.C. Mayur, Cytotoxicity studies of some novel fluoro acridone derivatives against sensitive and resistant cancer cell lines and their mechanistic studies, *European Journal of Pharmaceutical Sciences* 43 (2011) 217–224.
- [14] V.V.S. Rajendra Prasad, J. Venkat Rao, R.S. Giri, N.K. Sathish, S.M. Shanta Kumar, Y.C. Mayur, Chloro acridone derivatives as cytotoxic agents active on multidrug resistant cell lines and their duplex DNA complex studies by electrospray ionization mass spectrometry, *Chemico-Biological Interactions* 176 (2008) 212–219.
- [15] R.A. Friesner, J.L. Banks, R.B. Murphy, T.A. Halgren, J.J. Klicic, D.T. Mainz, M.P. Repasky, E.H. Knoll, M. Shelley, J.K. Perry, D.E. Shaw, P. Francis, P.S. Shenkin, Glide: a new approach for rapid, accurate docking and scoring. 1. Method and assessment of docking accuracy, *Journal of Medicinal Chemistry* 47 (2004) 1739–1749.
- [16] R.A. Friesner, R.B. Murphy, M.P. Repasky, L.L. Frye, J.R. Greenwood, T.A. Halgren, P.C. Sanschagrin, D.T. Mainz, Extra precision glide: docking and scoring incorporating a model of hydrophobic enclosure for protein–ligand complexes, *Journal of Medicinal Chemistry* 49 (2006) 6177–6196.
- [17] T. Hou, J. Wang, Y. Li, W. Wang, Assessing the performance of the MM/PBSA and MM/GBSA methods. 1. The accuracy of binding free energy calculations based on molecular dynamics simulations, *Journal of Chemical Information and Modeling* 51 (2011) 69–82.
- [18] P.D. Lyne, M.L. Lamb, J.C. Saeh, Accurate prediction of the relative potencies of members of a series of kinase inhibitors using molecular docking and MM-GBSA scoring, *Journal of Medicinal Chemistry* 49 (2006) 4805–4808.
- [19] J.C. Shelley, A. Cholleti, L.L. Frye, J.R. Greenwood, M.R. Timlin, M. Uchimaya, Epik: a software program for pK_a prediction and protonation state generation for drug-like molecules, *Journal of Computer-Aided Molecular Design* 21 (2007) 681–691.
- [20] QikProp, version 3.5, Schrödinger, LLC, New York, NY, 2012.
- [21] A. Cavalli, E. Poluzzi, F. De Ponti, M. Recanatini, Toward a pharmacophore for drugs inducing the long QT syndrome: insights from a CoMFA study of HERG $K(+)$ channel blockers, *Journal of Medicinal Chemistry* 45 (2002) 3844–3853.
- [22] M. Yazdani, S.L. Glynn, J.L. Wright, A. Hawi, Correlating partitioning and caco-2 cell permeability of structurally diverse small molecular weight compounds, *Pharmaceutical Research* 15 (1998) 1490–1494.
- [23] J.M. Luco, Prediction of the brain–blood distribution of a large set of drugs from structurally derived descriptors using partial least-squares (PLS) modeling, *Journal of Chemical Information and Computer Science* 39 (1999) 396–404.
- [24] J.D. Irvine, L. Takahashi, K. Lockhart, J. Cheong, J.W. Tolan, H.E. Selick, J.R. Grove, MDCK (Madin–Darby canine kidney) cells: a tool for membrane permeability screening, *Journal of Pharmaceutical Sciences* 88 (1999) 28–33.
- [25] R.O. Potts, R.H. Guy, Predicting skin permeability, *Pharmaceutical Research* 9 (1992) 663–669.
- [26] G. Colmenarejo, A. Alvarez-Pedraglio, J.L. Lavandera, Cheminformatic models to predict binding affinities to human serum albumin, *Journal of Medicinal Chemistry* 44 (2001) 4370–4378.
- [27] J. Kelder, P.D. Grootenhuys, D.M. Bayada, L.P. Delbressine, J.P. Ploemen, Polar molecular surface as a dominating determinant for oral absorption and brain penetration of drugs, *Pharmaceutical Research* 16 (1999) 1514–1519.
- [28] S.L. Dixon, A.M. Smondyrev, E.H. Knoll, S.N. Rao, D.E. Shaw, R.A. Friesner, PHASE: a new engine for pharmacophore perception, 3D QSAR model development, and 3D database screening: 1. Methodology and preliminary results, *Journal of Computer-Aided Molecular Design* 20 (2006) 647–671.
- [29] A. Golbraikh, A. Tropsha, Beware of q^2 !, *Journal of Molecular Graphics and Modelling* 20 (2002) 269–276.
- [30] P. Lu, X. Wei, R. Zhang, CoMFA and CoMSIA 3D-QSAR studies on quionolone carboxylic acid derivatives inhibitors of HIV-1 integrase, *European Journal of Medicinal Chemistry* 45 (2010) 3413–3419.
- [31] A. Basu, K. Jasu, V. Jayaprakash, N. Mishra, P. Ojha, S. Bhattacharya, Development of CoMFA and CoMSIA models of cytotoxicity data of anti-HIV-1-phenylamino-1H-imidazole derivatives, *European Journal of Medicinal Chemistry* 44 (2009) 2400–2407.
- [32] W.Y. Cheung, Properties of cyclic 3',5'-nucleotide phosphodiesterase from rat brain, *Biochemistry* 6 (1967) 1079–1087.